INTERNATIONAL JOURNAL OF GEOMAGNETISM AND AERONOMY
VOL. 6, GI1001, doi:10.1029/2004GI000083, 2005

Longitudinal variations of the electron concentration in the ionospheric *D* region

G. V. Givishvili, and R. V. Pisarev

Institute of Terrestrial Magnetism, Ionosphere, and Radio Wave Propagation, Troitsk, Moscow Region, Russia

Received 8 June 2004; revised 1 February 2005; accepted 2 May 2005; published 20 September 2005.

[1] Analysis of the longitudinal effects in the lower ionosphere revealed from the measurements by rockets and partial reflection method is presented. It is shown that in the summer and equinox periods the electron concentration in the altitude range 70–85 km at fixed zenith angle varies by a factor of 1.5–5.6 at the transition from the Pacific longitudinal sector to the Eurasian and American sectors. The longitudinal effects depend on season and time of the day: they are weak in the American sector and strong in the Eurasian sector. A conclusion is drawn that to reconstruct the longitudinal features of the global structure of the lower ionosphere, it is reasonable to attract the data obtained by the A1 method.
INDEX TERMS: 2447 Ionosphere: Modeling and forecasting; 2443 Ionosphere: Midlatitude ionosphere; 2494 Ionosphere: Instruments and techniques; *KEYWORDS:* Ionospheric *D* region; Empirical modeling; Electron concentration.

Citation: Givishvili, G. V., and R. V. Pisarev (2005), Longitudinal variations of the electron concentration in the ionospheric *D* region, *Int. J. Geomagn. Aeron., 6,* GI1001, doi:10.1029/2004GI000083.

1. Introduction

[2] Currently, there exist a few versions of empirical models of the lower ionosphere in this or that way taking into account the dependence of the electron concentration (n_e) at 60–90 km on solar and geomagnetic activity, latitude, season, and local time [*Belikovich et al.*, 1983; *Bilitza*, 1990; *Bremer and Singer*, 1977; *Danilov and Ledomskaya*, 1983; *Danilov et al.*, 1991; *Chasovitin*, 1983; *Friedrich and Torkar*, 1992, 2001; *Knyazev et al.*, 1993; *McNamara,* 1979]. However, the discrepancies between these models in a description of the above indicated dependencies even in quiet solar and geomagnetic conditions of middle and lower latitudes are so strong that the question on the causes of the discrepancies is inevitable. As one of such causes, *Danilov et al.* [1991] considered meteorological effects of the winter anomaly (WA) and stratospheric warmings (SW). Both these phenomena influence strongly and in the opposite directions the structure of the midlatitude lower ionosphere in winter months. Another possible source of the systematic discrepancy between the above indicated models is the longitudinal effect. The role of this effect in formation of the global structure of the *D* region was considered only in the *McNamara* [1979] model. At the same time, the satellite measurements of nitric oxide in the lower thermosphere indicate to a relation of [NO] at a height of 105 km not only to the geographic latitude, but to the geomagnetic latitude as well [*Gravens and Stewart*, 1978]. Bearing in mind that NO is the main ionized agent (actually a source of the *D*-region formation) and that its content in this region evidently is determined by the vertical transport, one can assume that longitudinal effects should also exist in the latitude–longitude structure of the lower ionosphere. To confirm this statement, one can refer to the results of the measurements of the ionospheric radio wave absorption by the A1 method conducted at the stations of the global network in the periods of IGY (International Geophysical Year) and IQSY (International Quiet Sun Year) [*Belkina*, 1968; *Bremer et al.,* 1980; *Fligel'*, 1962; *George*, 1971; *Ginzburg and Nesterova*, 1974; *Givishvili*, 1976; *Schwentek*, 1976; *Shirke and Henry*, 1967]. One should bear in mind that the A1 method provides a rough enough representation of the n_e vertical profile and characterizes mainly the integral content of electrons in the column from the bottom of the ionosphere to the reflection point of the sounding signals located (most often) in the *E* region. The difficulties of reconstruction of the n_e vertical profile we are going to eliminate in the following way. Finding a dependence of n_e on these or that geophysical conditions in the altitude range 65–95 km, to fit the obtained $n_e(h)$ profiles of the *D* region to the $n_e(h)$ profiles in the *E* layer, the spatial and time variations of the latter being

1524–4423/05/2004GI000083$18.00

studied with a high degree of accuracy and reliability. Using the obtained in such a way vertical profiles of n_e and the data on the vertical distribution of the neutral atmosphere density (electron collision frequencies), values of the integral absorption L (in dB) at frequencies used for the measurements by the A1 method at this or that station are calculated. The choice of the $n_e(h)$ profile corresponding to the corresponding analyzed solar and geophysical conditions is performed by the method of minimization of the difference between the calculated and measured values of L.

[3] The aim of the first part of this paper is to specify the regularities in the spatial-time structure of the lower ionosphere in the latitude interval 66°N–59°S on the basis of the data obtained mainly in rocket measurements (R) and by the partial reflection method (PR).

2. Analysis of the Available Models

[4] *Belikovich et al.* [1983] used as initial data for creation of the model the original results of the measurements by the PR method for the period 1969–1980 and also the results of the measurements by the PR and cross-modulation methods, as well as in rocket experiments published in literature (totally about 500 measurements). The variations in the electron concentration with solar zenith angle (χ), season, and solar activity (the Wolf number, W) were described by

$$n_e(h) = n_e(h)_0 \cos^{p(h)} \chi_{\text{eff}} \times$$

$$\left[1 + k(h) \cos\left(2\pi \frac{m - 91}{365}\right)\right] e^{\alpha(h) R}$$

where the initial height is $h_0 = 60$ km, $p = 0.5 - 0.9$, $\alpha = -0.008 \div 0.012$ depending on h, m is the number of days counted from 21 March. The coefficient k determining the seasonal variations of $n_e(h)$ is positive at heights of 60–80 km and negative at heights of 85–95 km. The model is applicable in the latitude range $\varphi = 30^\circ - 60^\circ$ at altitudes 60–95 km in the sunlit period of a day, and in quiet geophysical conditions. The *Danilov et al.* [1991, 1995] model was created on the basis of the database including 276 profiles with n_e values at altitudes of 60–85 km obtained by various rocket methods during the period from 1948 to 1978 in the latitude interval 81°N–30°S. The model makes it possible to calculate the values of $n_e(h)$ in the lower ionosphere depending on χ, season (S) and geomagnetic index (Kp). The model takes into account the meteorological effects: the winter anomaly events and stratospheric warmings according to

$$\log n_e = A_0 + A_1 f(\chi) + A_2 f(Kp) + A_3 f(\text{S}) +$$

$$A_4 f(\text{SW}) + A_5 f(\text{WA})$$

where $A_0 - A_5$ are the coefficients different for different altitudes (with a step of 5 km) determining variations depending on each of the parameters taken into account. The global model by *Chasovitin* [1988] is created for the 80–600 km range, however below 200 km the electron concentration is calculated using the *Chasovitin* [1983] model. The latter may be used for the conditions of moderate solar activity ($100 \le F_{10.7} \le 150$) and quiet geomagnetic situation ($Kp \le 4$). The model is presented in the form of tables calculated for each variation in the input parameters. The *Bilitza et al.* [1981] model was a basis for the description of the dependency of the undisturbed lower ionosphere structure on the time of a day (day–night), solar zenith angle, and solar activity in the models IRI 1979, 1990, 1995/96, and 2001. The model considers only rocket measurements (about 80). The vertical profile of ne is approximated by the polynomial of the third degree centered above and below the inflection point located at a height of $h = 81$ km. Two latitudinal intervals are considered: the lower and middle (however the differences between them are negligible). It is shown that the value of n_e in the inflection point may be given by

$$n_e = (6.05 + 0.088 R_{12}) 10^2 e^{(0.1/\cos \chi^{27})}$$

where R_{12} is the running mean (over 12 years) Wolf number. The *Pancheva and Mukhtarov* [1997] model was created on the basis of the measurements of the radio wave absorption obtained by the A3 method. The data obtained only in Bulgaria were used, so the model does not provide the global structure of the lower ionosphere. Nevertheless the model analyzes in detail diurnal and seasonal variations of n_e. The model profile $n(h)$ is presented in some set of characteristic points connected by cubic splines to provide the continuity of the profile. The values of n_e are determined unambiguously only in the characteristic points and the variations of the $n_e(h)$ profile with χ, $F_{10.7}$, and season are modeled changing the values of n_e in these characteristic points. *Friedrich and Torkar* [1992] actually described in their model only the dependence of the electron concentration on the solar zenith angle. This was due to the very limited database of the initial data (72 profiles obtained by the rocket method). The model is created for moderate solar activity ($W = 60$), middle latitudes and undisturbed geomagnetic conditions. *McNamara* [1979] collected and analyzed about 700 profiles of ne obtained mainly by rocket methods and PR methods. This publication is the only one in which an attempt is made to take into account the longitudinal effects in the lower ionosphere mentioned earlier by *George* [1971] and *Mechtly et al.* [1969]. However, the longitudinal effects in the *McNamara* [1979] model are taken into account in the latitudinal dependence of n_e due to the difference in the measurement points of geographic (φ) and geomagnetic (θ) latitudes as well as of the modified dipole latitude $X = \arctan(I/\cos\varphi)$. The expression for the electron concentration at the given height is presented by the linear function:

$$\log n_e = A_0 + A_1 \cos \chi + A_2 f_1(\sin \theta) + A_3 W +$$

$$A_4 \cos\left(2\pi \frac{M - 0.5}{12}\right) + A_5 f_2(Kp)$$

where M is the number of the month.

Table 1. Mean Values of the Electron Concentration and Its Standard Deviations

Height, km	Winter				Summer			
	Rocket		PR		Rocket		PR	
	$\log(\tilde{n}_e)$	$\sigma(\log(\tilde{n}_e))$	$\log(\tilde{n}_e)$	$\sigma(\log(\tilde{n}_e))$	$\log(\tilde{n}_e)$	$\sigma(\log(\tilde{n}_e))$	$\log(\tilde{n}_e)$	$\sigma(\log(\tilde{n}_e))$
60	1.39	0.44	1.97	0.74	1.29	0.40	1.82	0.41
65	1.70	0.28	2.03	0.73	1.71	0.29	2.18	0.29
70	2.20	0.28	2.20	0.48	2.15	0.43	2.34	0.28
75	2.56	0.32	2.48	0.36	2.53	0.39	2.48	0.29
80	3.00	0.40	2.85	0.36	2.73	0.34	2.75	0.29
85	3.47	0.40	3.36	0.36	3.11	0.46	3.13	0.39
90	3.90	0.32	3.70	0.36	3.82	0.43	3.62	0.47

3. Creation of an Alternate Model

[5] The problem of revealing and description of the dependence of the modeled parameter on input conditions may be solved using different approaches. Currently three methods of solution of this problem are available. The first includes a statistical treatment of the experimental data and drawing of the electron concentration dependence on various input parameters in the table form or creating typical n_e vertical profile for the chosen characteristic conditions. This approach has its defects: low flexibility of the model, large averaging over the input parameters, and too approximate splitting of these parameters (for example, a simple separation of solar activity to "high" and "low"). The second method is based on description of the entire $n_e(h)$ vertical profile which is some continuous function including as arguments such parameters as φ, χ, S, $F_{10.7}$ (or W), and others. Any change in the arguments leads to a change in the entire profile.

[6] The third method is based on representation of n_e values at some fixed height by a functional depending on different physical input parameters. Usually the functional is linear relative the input parameters and gives values of n_e at a fixed height as a sum of model functions each depending on one (more seldom, on several) input parameters. To obtain the general model, several such functionals (key points) with a fixed step (e.g., 5 km) are formed in such a way that the n_e behavior at these heights would most adequate represent the behavior of the entire $n_e(h)$ profile. Some characteristic points (maximum, minimum, inflection point) may be also chosen as key point. Thus, for the same given input parameters, there are several different by height key points. Approximating these points by some polynomial one can obtain a continuous $n_e(h)$ profile. In this paper we used the latter method of model creation. For each chosen height an expression was written, its coefficients being found by the multiple regression method.

[7] The database of experimental data used in this paper consists of the measurements of n_e in middle and lower latitudes at undisturbed solar and geophysical conditions compiled by *Nesterova and Ginzburg* [1985] and *Belikovich et al.* [1983]. For the profiles for which in the databases there was no information on χ, Kp, or $F_{10.7}$ the corresponding parameters were calculated on the basis of the geographical coordinates (φ, λ) and local time (LT). Obviously, erroneous profiles and profiles strongly different from the statistical series (the causes of the latter were, as a rule, disturbed conditions not indicated in the catalogs) were rejected. On the whole the database contained: 236 profiles obtained by rocket methods, 450 profiles obtained by the partial reflection method, and 59 profiles derived from the data on LF and VLF radio wave reflection (the A3 method) for the period 1948–1984. Because of the presence of considerable seasonal variations in n_e the data were split into three subsets corresponding to winter (November, December, January, and February), equinox (March, April, September, and October), and summer (May, June, July, and August). Assuming the existence of considerable longitudinal effects we split the data on n_e into three groups corresponding to the following longitudes: $\lambda = 340^\circ - 100^\circ$ (Eurasia), $\lambda = 100^\circ - 220^\circ$ (Oceania), and $\lambda = 220^\circ - 340^\circ$ (America).

[8] Since the main part of the database consists of the measurements conducted by two methods (rocket and PR) with different accuracy characteristics, a comparative analysis of these two groups was performed. Table 1 shows the values of $\log \tilde{n_e}$ and their standard deviations σ for winter and summer. Figure 1 shows the values of $\Delta = \log(\tilde{n}_e)_\mathrm{r} - \log(\tilde{n}_e)_\mathrm{pr}$ for winter, summer, and equinox (in this case to increase the statistical reliability of the analysis results no separation on longitudes was done). One can see that below 67.5 km the values of Δ are comparable to and even higher than the standard deviations σ. As far as we have no ground to prefer any of the considered methods, the further analysis was performed for $h \geq 70$ km. (Thus the C layer is out of the further consideration). Moreover, the data of both groups above 67.5 km may be considered as coinciding only in equinoxes. In summer and winter the PR method gives, respectively, overestimated and underestimated values of n_e as compared to the data of rocket measurements. Nevertheless the discrepancies lie within the measurement errors. Therefore, analyzing the n_e dependencies on various solar and geophysical conditions, the data of rocket measurements and measurements by the PR method may be considered jointly as one database. One should note, however, that above 85 km in winter and equinoxes the discrepancy between the two methods begins to increase again. So to minimize the errors re-

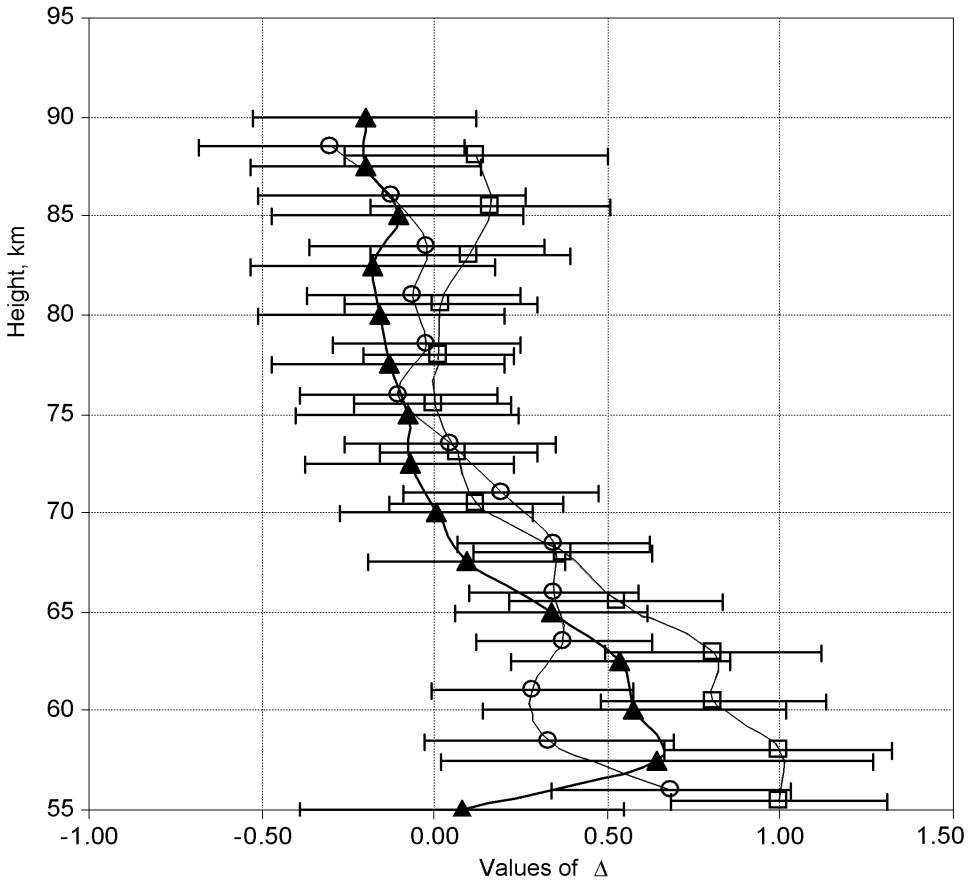

Figure 1. $\Delta = \log(n_e)_{\rm r} - \log(n_e)_{\rm pr}$ for winter (triangles), equinox (circles), and summer (squares), and corresponding standard deviation σ.

lated to nonhomogeneity of the used data the range of the considered height was taken to be 70–85 km.

4. Data Analysis

4.1. Longitudinal Variations

[9] Figures 2–4 show the results of measurements at altitudes of 75–85 km at solar zenith angles $45^\circ \le \chi \le 60^\circ$ and $60^\circ \le \chi \le 90^\circ$ in the summer and equinox periods. One can see a small number and irregularity in the spatial distribution of the measurement points do not make it possible to reconstruct the fine structure of the longitudinal behavior of n_e. Nevertheless, even at such unfavorable for the given analysis conditions, deviations from the zonal mean values are clearly manifested in the longitudinal behavior of n_e. These deviations show a pronounced minimum in the longitudinal behavior of n_e falling on the Pacific longitudinal sector. Approximating the longitudinal behavior of n_e by a periodic function, we obtain that at $h = 75$ km the ratio $l = n_e^{\max}/n_e^{\min} = 3.8 - 4.7$, where the indices max and min refer to the electron concentrations in the vicinity of longitudes $\lambda = 340^\circ$ and 160°, respectively. At $h = 80$ km and 85 km $l = 1.5 - 5.6$ and $l = 3 - 3.3$, respectively. The longitudinal dependence of n_e at the zenith angles $\chi \ge 60^\circ$, as a rule, is less pronounced than at $\chi \le 60^\circ$. One should note that the extremes in the longitudinal distribution of n_e demonstrate some relation to the spatial structure of the NO at $h = 105$ km which is governed by the dipole latitude. The dip equator in Figures 2–4 is shown by solid curve. According to *Gravens and Stewart* [1978] the maximum and minimum of [NO] at middle latitudes of the northern hemisphere fall on the longitudes $\lambda = 280^\circ - 300^\circ$ and $\lambda = 100^\circ - 120^\circ$, respectively. One can see in Figures 2–4 that the maximum in the longitudinal behavior of n_e is actually located close to $\lambda = 280^\circ - 300^\circ$. As for the minimum in the longitudinal behavior of n_e it is shifted to $\lambda = 160^\circ - 180^\circ$. This fact is, most probably, explained by the absence of enough measurement data in the Oceania longitudinal sector.

4.2. Dependence on Local Time

[10] The least deviations between the available lower ionosphere models are in the dependence of the shape of the $n_e(h)$ profile on local time. Nevertheless they still exist. For

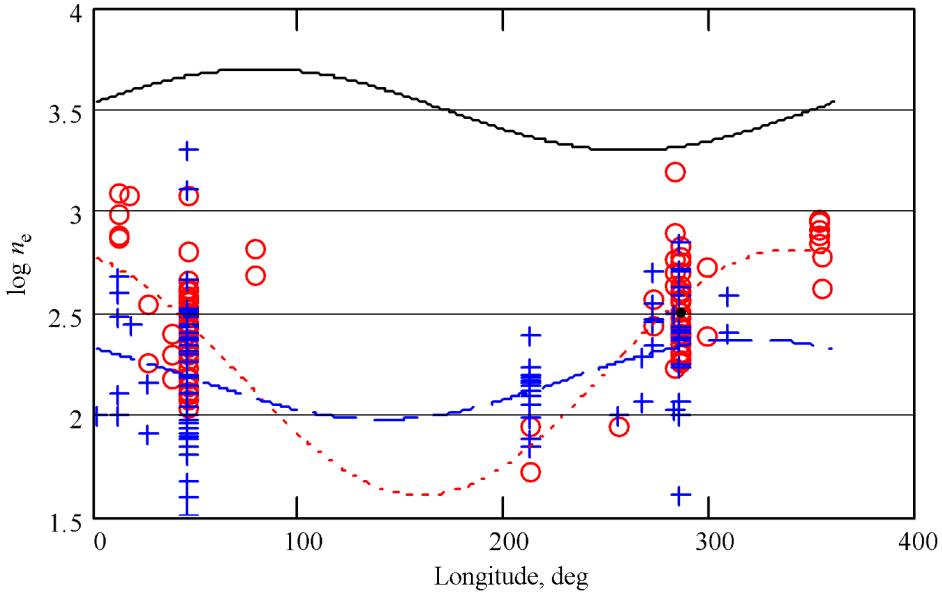

Figure 2. Longitudinal behavior of n_e at a height of 75 km for $45° < \chi < 60°$ (circles, dotted line) and $60° < \chi < 90°$ (crosses, dashed line) and also for the dip equator (solid curve).

example, the value of $n(h)$ for $\chi \leq 70°$ in the IRI model has the maximum value at a height of 65 km, whereas according to *Belikovich et al.* [1983] the maximum is located at a height of 90 km. *Knyazev et al.* [1993] performed a comparative analysis of the expression for $n_e(h)$ presented in the IRI with their own data. They came to the conclusion that the discrepancies between their results and the data tabulated in IRI at some altitudes reach 100%. *Danilov and Smirnova* [1994] showed that the $n_e(h)$ dependency on χ postulated in IRI is not confirmed by the experimental data for $\chi > 70°$.

An alternate description of the $n_e(h)$ dependency on χ was proposed in the *Danilov et al.* [1991] model:

$$f(\chi) = A(h)\cos^{0.5}\chi \qquad \chi \leq 90$$

where the $A(h)$ coefficient is tabulated. However, again according to the conclusions of *Knyazev et al.* [1993] the *Danilov et al.* [1991] model values of n_e are underestimated as compared to the empirical data up to an order of

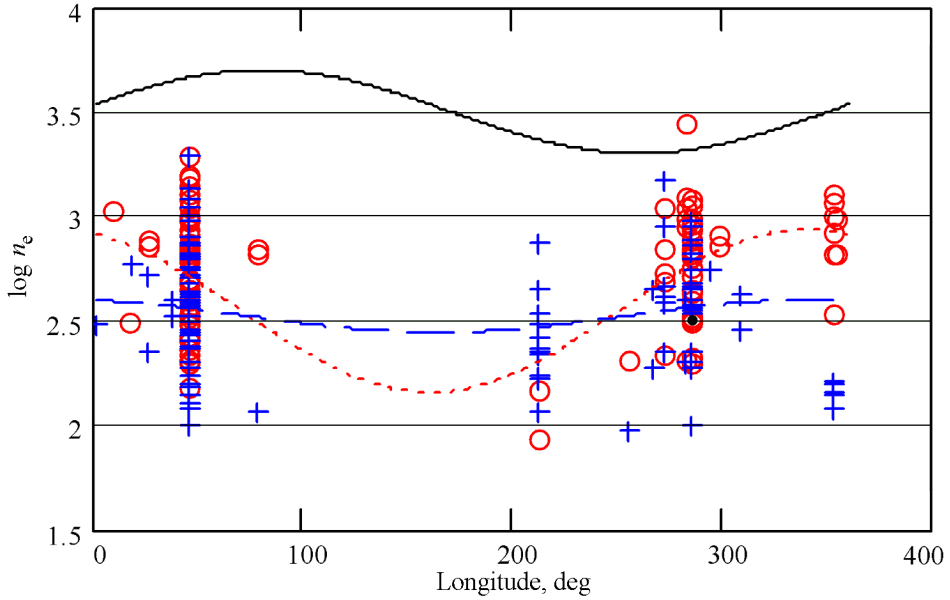

Figure 3. Same as in Figure 2, but for a height of 80 km.

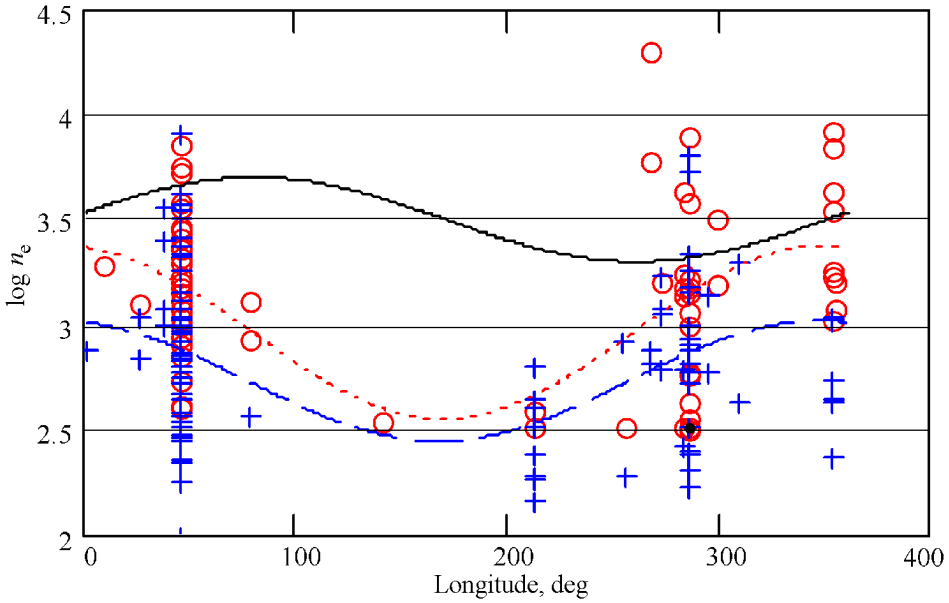

Figure 4. Same as in Figure 2, but at a height of 85 km.

magnitude. An attempt to analyze the diurnal behavior of n_e on the basis of the absorption measurements by the A3 method was made by *Pancheva and Mukhtarov* [1997]. This model shows that in winter at heights below 60 km n_e is subject to no changes with the decrease of $\cos\chi$. At altitudes 65 km and 85 km n_e increases linearly toward the noon, whereas at a height of 70 km the n_e dependence on $\cos\chi$ have a pronounced nonlinear character. For summer conditions the picture stays nearly the same, but at heights of 65 km and 80 km the dependence becomes of a power character and at 70 km it becomes even more complicated.

[11] The results of our analysis for 80 km performed separately for the Eurasian and American longitudinal sectors are shown in Figure 5. One can see that the n_e dependence on χ in these sectors is significantly different. Similar difference takes place also at heights of 75 km and 85 km. Figure 5 shows also the approximating curve of the $\log n_e(\chi)$ dependence from the IRI model for the middle of the American

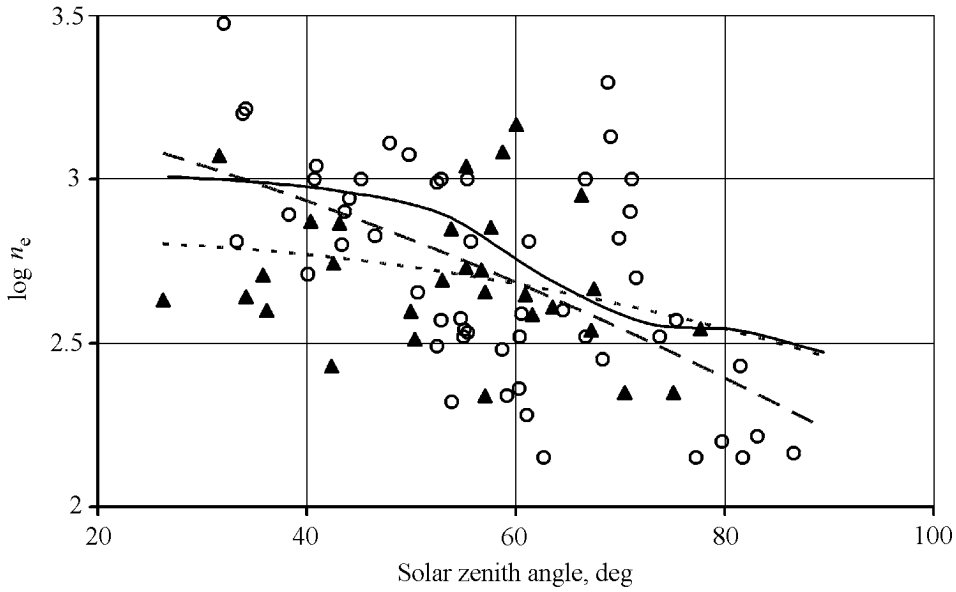

Figure 5. Dependence of n_e on χ at 80 km for moderate solar activity ($100 < F_{10.7} < 150$), middle latitudes, and summer time for Eurasia (circles, dashed curve) and America (triangles, dotted curve). Solid line shows the IRI model for $\varphi = 50°$, $F_{10.7} = 125$ ($W = 70$), and $\lambda = 280°$.

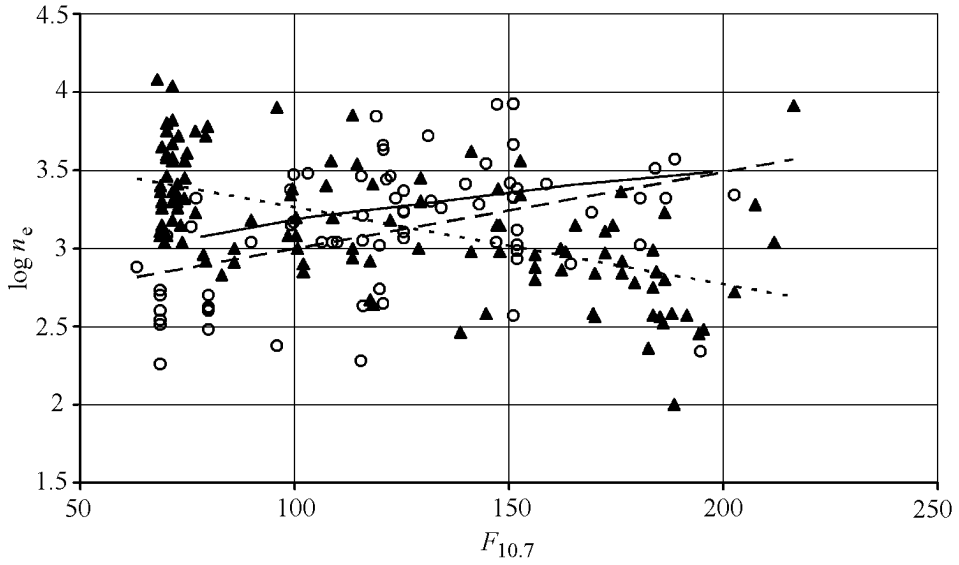

Figure 6. Dependence of n_e on $F_{10.7}$ at 85 km for the Eurasian region: rocket data (circles, dashed line), PR method (triangles, dotted line). Solid line corresponds to the IRI model for 1980–1985 and $\chi = 50°$.

($\lambda = 280°$) and Eurasian ($\lambda = 40°$) longitudinal sectors. One can see that the $\log n_e(\chi)$ dependence from the IRI demonstrates no longitudinal features. On the other hand, at the solar zenith angles $\chi \leq 60°$ it is close to the $\log n_e(\chi)$ dependence for the Eurasian region and at the angles $\chi \geq 60°$ the dependence is close to the $\log n_e(\chi)$ curve for the American region.

4.3. Relation to the Solar Activity Level

[12] A compilation of the dependencies of the shape of $n_e(h)$ profiles on solar activity obtained by different authors was presented by *Danilov* [1998]. The compilation shows that there are considerable differences in this shape. For example, the ratio $r = n_e^{\mathrm{h}}/n_e^{\mathrm{l}}$, where the indices "h" and "l" correspond to high and low solar activity, respectively, at a height of 60 km vary according to different authors from 0.3 to 1.6, that is by a factor of more than 5. This ratio at 70 km and 80 km varies within 0.9–2.6 and 1.0–3.6, respectively. Only at 90 km the scatter of the ratio in question decreases down to the range 1.2–2.0. The directly opposite conclusion was drawn by *Bremer and Singer* [1977]. On the basis of the data of ionospheric radio wave absorption they claimed that the effect of the solar activity impact (while $F_{10.7}$ changed from 75 to 150) on the electron concentration may be considered negligible small at all altitudes in the range 60–100 km. However, the vertical structure of the n_e distribution is almost identical in both publications. The ratio r in the *Bilitza* [1990] model is taken equal to 1.9–2.0 for altitudes of 70–90 km, whereas *Danilov et al.* [1991] accepted $r = 1$ because the available material did not make it possible to detect any n_e dependence on $F_{10.7}$.

[13] The allowance for the influence of the longitudinal effects on the $\log n_e(F_{10.7})$ dependence made it possible to reveal an astonishing fact. Figure 6 shows separately the results of the measurements obtained by rockets and PR method in the Eurasian region. The corresponding dependence from the IRI model for similar solar and geomagnetic conditions is also presented. One can see that the dependence from IRI is close to the $\log n_e(F_{10.7})$ dependence obtained on the basis of rocket data but is opposite to the dependence obtained on the basis of the PR data. This inverse relation between n_e and $F_{10.7}$ revealed on the basis of the PR measurements in the Eurasian sector is especially astonishing because it is direct in the American sector as one can see in Figure 7. The explanation to this fact should be looked for in peculiarities of the method used in the PR measurements by the *Belikovich et al.* [1983] group. Their data present the major part of the set of measurements by PR method in the Eurasian sector. In favor of this conclusion is the fact that the $n_e(F_{10.7})$ dependence presented in their paper was based only on the data obtained by rockets. At the same time the question on the cause of the appearance of such unusual reaction of this group of measurements to variations in solar activity needs a special consideration what is out of the scope of this paper. Here we emphasize the fact that everywhere according to the results of rocket measurements and in the American longitudinal sector according to the measurements by the PR method the relation of n_e to $F_{10.7}$ may be presented by the linear formula of the type:

$$\log n_e(h) = A_0(h) + A_1(h)F_{10.7}$$

4.4. Seasonal Variations

[14] The strong variability of the $n_e(h)$ profile in winter

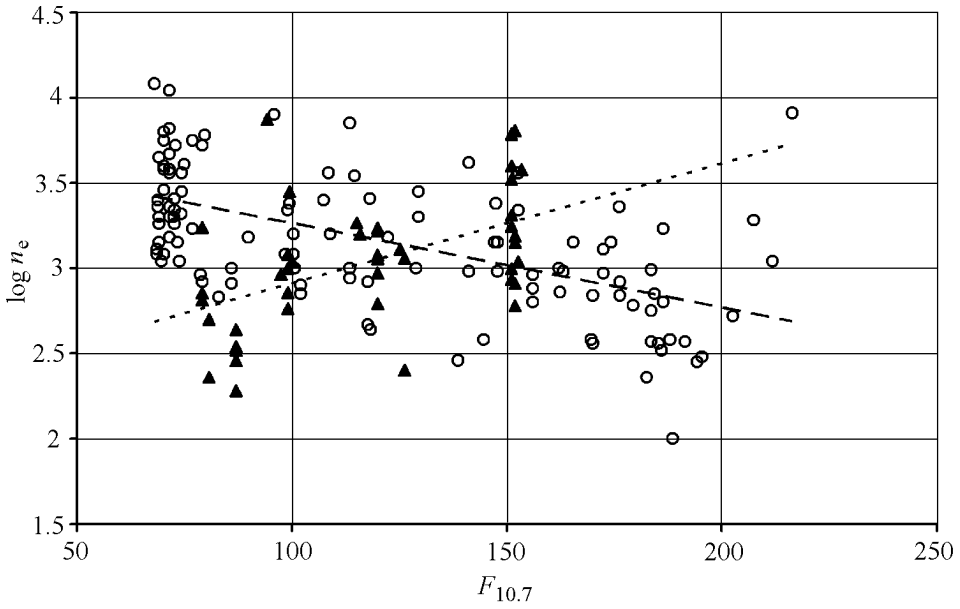

Figure 7. PR data at 85 km for the Eurasian (circles, dashed curve) and American (triangles, dotted curve) regions.

period often leads to a distortion of the n_e diurnal behavior in the major part of the D region and considerably complicates its description. Therefore currently, modeling the winter anomaly of the lower ionosphere on the whole, it is reasonable to consider some general tendencies of the dependence of the $n_e(h)$ profile features on the season, bearing in mind that the profile for each particular moment may differ considerably from the mean one. This makes it clear why out of all the models considered above the winter anomaly is taken into account only in the *Danilov et al.* [1991] and *Pancheva and Mukhtarov* [1997] models. In the former publication the phenomenon is considered discretely: "no WA", "weak WA", and "strong WA". The corresponding function entering the expression for $\log(n_e)$ takes the values 0, 0.5, and 1, and the value of the coefficient A5 at the function varies from 0.1 at a height of 65 km to 0.7 at a height 90 km and 1.0 at heights of 80 km and 85 km. Moreover, the model takes into account such events as stratospheric warmings (SW) leading to a decrease of n_e at altitudes of the D region rather than to an increase. This factor is also divided at three steps: "no SW", "weak SW", and "strong SW". The effect of WA in the *Pancheva and Mukhtarov* [1997] model is described in a slightly different way. In this model the electron concentration at the same values of χ is subjected to only weak variations in different seasons. At the same time in the $n_e(h)$ profiles an additional intermediate layer is clearly seen at altitudes of 55–65 km. The IRI model also demonstrates no significant seasonal variability of n_e at fixed solar zenith angles χ (see Table 2).

[15] Our analysis for the Eurasian and American regions (the results are shown in Figures 8 and 9) indicates to a strong and weak seasonal variability of n_e at $60^\circ \le \chi \le 75^\circ$ and $75^\circ \le \chi \le 90^\circ$ in the former and latter longitudinal sectors, respectively. One can see, for example, that in the Eurasian sector the winter values of n_e at the same zenith angles χ exceed the summer ones by about a factor of 5. Similar difference between the winter and summer values of n_e exists at altitudes of 75 km and 85 km. No such difference is detected in the American sector. To clarify the problem of possible relation of the seasonal effect in the Eurasian region to the peculiarities of the PR method, we show in Figure 10 separately the results of the measurements at a height of 80 km by this method and by rockets. One can see that the anomalous character of the seasonal variations of n_e cannot be explained by the peculiarities of the PR method, because the amplitude of the seasonal variations corresponding to the rocket measurements is almost by a factor of 2 higher than the amplitude of the same variations according to the PR

Table 2. Values of n_e According to the IRI Model at a Height of 80 km for 1973 at $\varphi = 50^\circ$ and $\lambda = 280^\circ$

Month	Local Time	χ	$\log n_e$
1	1354	74.7	2.568
2	1518	74.3	2.561
3	1621	74.5	2.555
4	1712	74.6	2.555
5	1751	74.7	2.557
6	1815	74.6	2.560
7	1812	74.8	2.558
8	1733	74.5	2.555
9	1630	74.5	2.555
10	1500	74.7	2.558
11	1357	74.6	2.566
12	1257	74.6	2.572

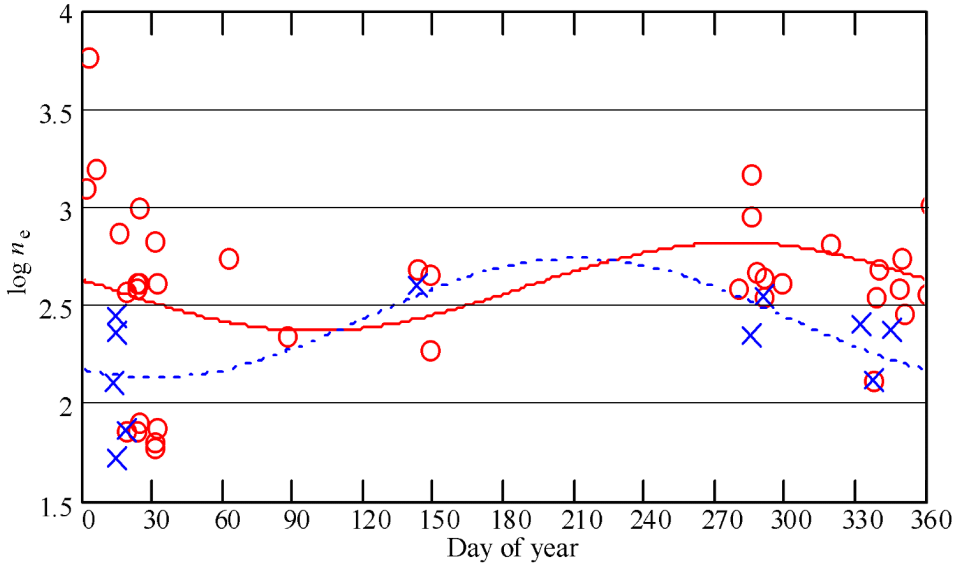

Figure 8. Seasonal behavior of n_e for the American region, for $60^\circ < \chi < 75^\circ$ (circles, solid curve) and $75^\circ < \chi < 90^\circ$ (crosses, dotted curve).

data. Therefore it follows that the location of the anomaly in the Eurasian region has a natural cause most probably related to the asymmetry of the mechanisms of horizontal and vertical transport influencing the nitric oxide content at heights of the D region. The annual behavior of n_e in the near-noon hours indirectly also indicate to this fact. The maximum of the electron concentration values in the summer and equinox periods falls on ~175 day of the year (the summer solstice, see Figure 11), whereas in the American sector it falls on ~110 day of the year (see Figure 12), that means it is in advance of the summer solstice by about 2 months.

4.5. Dependence on Geomagnetic Activity

[16] According to *Danilov et al.* [1991] the increase of the Kp index from 0 to 2 units leads at altitudes of 70–85 km to an increase of $\log n_e$ by 0.1–0.2 and stays unchanged with further increase of Kp. However, it is noted that the problem of the dependence of n_e in the D region on geomagnetic conditions needs further consideration. In the other models it is accepted that this dependence is so weakly pronounced that one can neglect it. According to our estimates the n_e dependence on geomagnetic activity has a value of minor corrections what may be neglected at all altitudes.

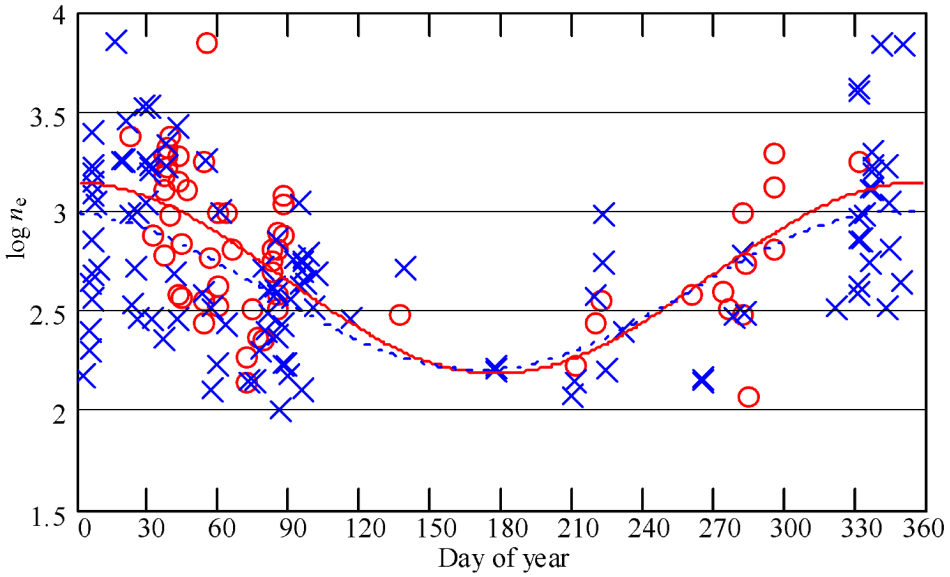

Figure 9. Seasonal behavior of n_e for the Eurasian region at 80 km for $60^\circ < \chi < 75^\circ$ (circles, solid curve) and $75^\circ < \chi < 90^\circ$ (crosses, dotted line).

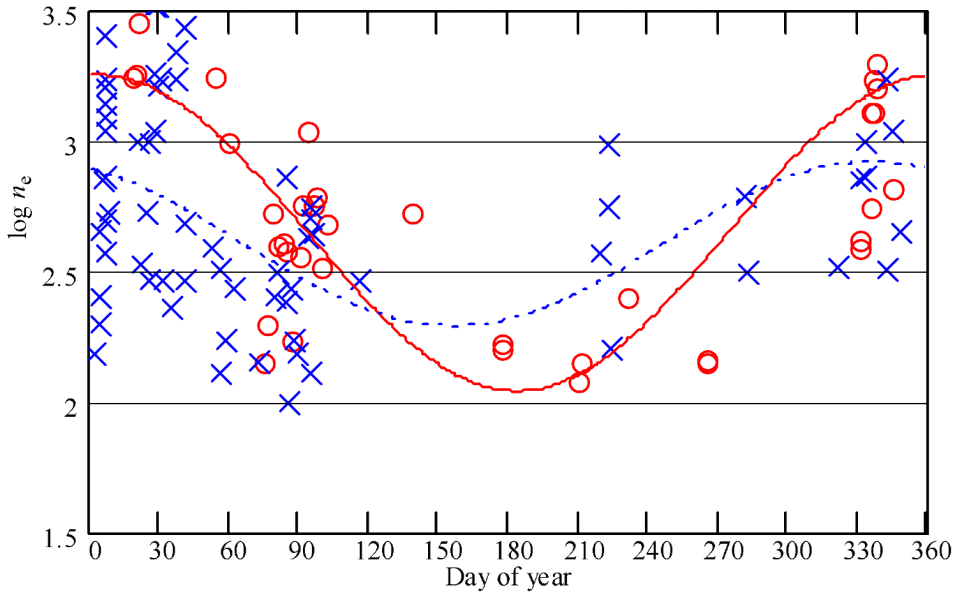

Figure 10. Seasonal behavior of n_e for the Eurasian region according to the rocket data (circles, solid curve) and PR measurements (crosses, dotted line).

5. Conclusions

[17] The presented analysis of the results of the n_e measurements by rockets and the partial reflection method makes it possible to draw the following conclusions.

[18] First, the assumption on the existence of peculiarities in the longitudinal behavior in the ionospheric D region is completely confirmed. The values of n_e at fixed heights and at fixed solar zenith angles vary by a factor of 1.5–5.6 at the transition from the Pacific to the Eurasian longitudinal sectors.

[19] Second, the longitudinal effects are manifested also in the seasonal behavior of n_e. The seasonal effects are weak and strong in the American and Eurasian sectors, respectively. In the latter sector the winter values of n_e at altitudes of 75–85 km exceed the summer values (at the same values of χ) by a factor of 4–6.

[20] Third, the longitudinal effects are manifested in the diurnal variations in n_e: at the variation of χ from 30° to

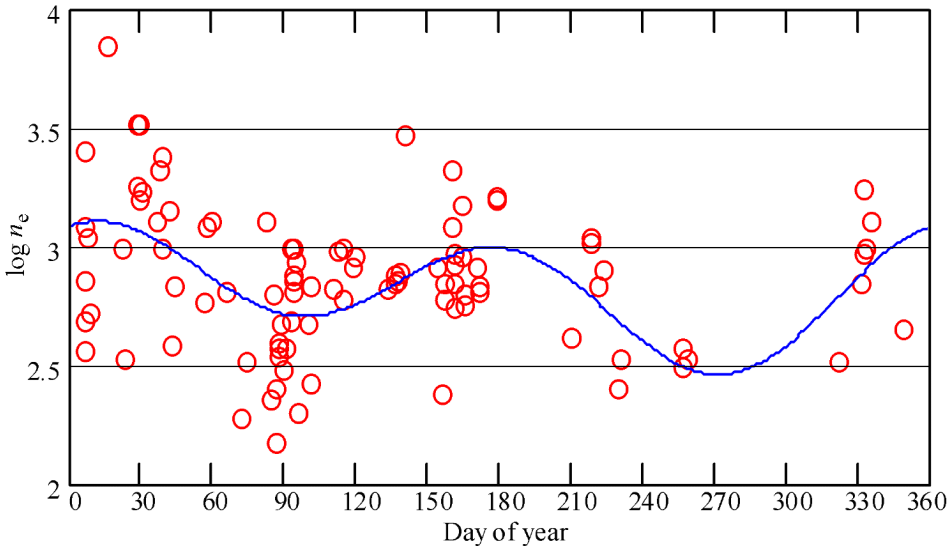

Figure 11. Annual behavior of n_e at a height of 80 km at noon at middle latitudes of Eurasia.

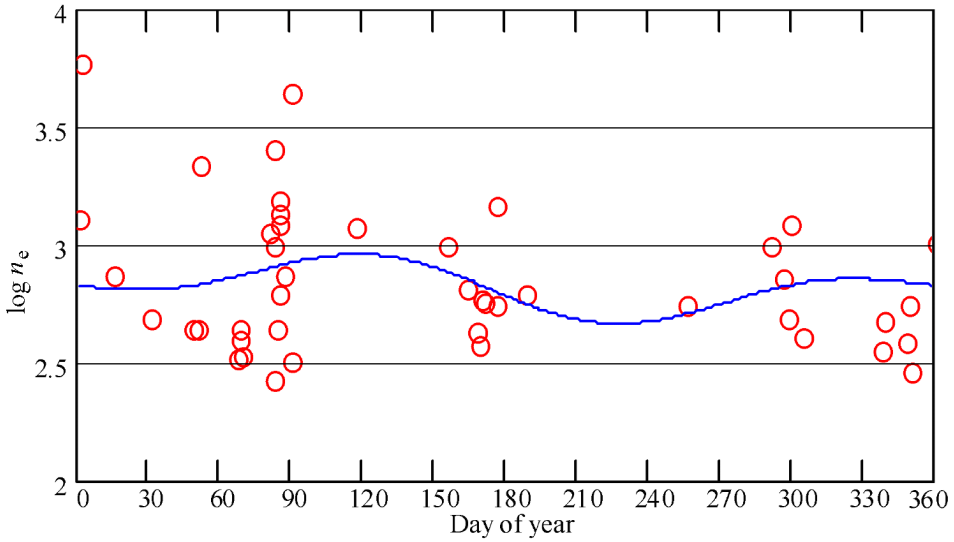

Figure 12. Same as in Figure 11, but for America.

90° the electron concentration decreases by a factor of about 2 and by a factor of 6 in the American and Eurasian sectors, respectively.

[21] Fourth, the longitudinal effects, apparently, are weakly manifested in the n_e dependence on solar activity.

[22] Fifth, the rocket measurements data and measurements by the PR method are comparable in the altitude range 75–85 km. Outside this range the difference between the two groups of data create considerable difficulties to their joint analysis.

[23] Sixth, the attraction of the data obtained by the A1 method for reconstruction of the fine structure of the empirical model of the global distribution of the lower ionosphere seems to be completely justified.

References

Belikovich, V. V., E. A. Benediktov, V. D. Vyakhirev, and L. V. Grishkevich (1983), Catalog of the electron concentration profiles in the *D* region of the midlatitude ionosphere, in *Development of the Principles of Creation of an Empirical Model, Preprint 171* (in Russian), p. 51, Radiophys. Res. Inst., Gorky, Russia.

Belkina, L. M. (1968), Spatial-time variations in the radio wave absorption in the ionosphere, *Geomagn. Aeron.* (in Russian), *8*(2), 309.

Bilitza, D. (1990), *International reference ionosphere 1990, WDC-A-R and 90-22,* Natl. Space Sci. Data Cent., Greenbelt, Md.

Bilitza, D., et al. (1981), Electron density in the *D* region as given by the International Reference Ionosphere, in *Report UAG 82,* p. 7–10, WDC-A-STP, Boulder, Colorado.

Bremer, J., and W. Singer (1977), Diurnal, seasonal and solar-cycle variations of electron densities in the ionospheric *D* and *E* regions, *J. Atmos. Terr. Phys., 39,* 25.

Bremer, J., H. Gernandt, and H. Lucke (1980), Global ionospheric absorption measurements on board ships, *Gerlands Beitr. Geophys., 89,* 81.

Chasovitin, Yu. K., Ed. (1983), *Reference Model of the Concentration, Temperature and Effective Collision Frequency of Electrons in the Ionosphere at Heights Below 200 km, report* (in Russian), Inst. of Exp. Mineral., Obninsk, Russia.

Chasovitin, Yu. K. (1988), Global empirical model of the distribution of the concentration, temperature, and effective collision frequency of electrons in the ionosphere, *Ionospheric Stud.* (in Russian), *44,* 6.

Danilov, A. D. (1998), Solar activity effects in the ionospheric *D* region, *Ann. Geophys., 16,* 1527.

Danilov, A. D., and S. Yu. Ledomskaya (1983), Creation of the empirical model of the *D* region, *Proc. Inst. Exp. Meteorol.* (in Russian), *13,* 28.

Danilov, A. D., and N. V. Smirnova (1994), Comparison of the International Reference Ionosphere to the rocket measurements, *Geomagn. Aeron.* (in Russian), *34*(6), 74.

Danilov, A. D., A. Yu. Rodevich, and N. V. Smirnova (1991), Parametric model of the *D* region taking into account meteorological effects, *Geomagn. Aeron.* (in Russian), *31*(5), 881.

Danilov, A. D., A. Yu. Rodevich, and N. V. Smirnova (1995), Problems with incorporating a new *D*-region model into the IRI, *Adv. Space Res., 15*(2), 165.

Fligel', M. D. (1962), Geographical distribution of ionospheric absorption, *Geomagn. Aeron.* (in Russian), *2*(6), 1091.

Friedrich, M., and K. M. Torkar (1992), An empirical model of the nonauroral *D* region, *Radio Sci., 27,* 945.

Friedrich, M., and K. M. Torkar (2001), FIRI: A semiempirical model of the lower ionosphere, *J. Geophys. Res., 106*(A10), 21,409.

George, P. L. (1971), The global morphology of the quantity $\int N\nu dh$ in the *D* and *E* regions of the ionosphere, *J. Atmos. Terr. Phys., 33,* 1893.

Givishvili, G. V. (1976), Spatial-time variations of the electron concentration in the lower ionosphere, *Geomagn. Aeron.* (in Russian), *16*(1), 92.

Ginzburg, E. I., and I. I. Nesterova (1974), Spatial-time variations in the $n_e(h)$ profiles in the lower ionosphere, in *Problems of Studies of the Lower Ionosphere and Geomagnetism* (in Russian), p. 3, Inst. of Geol. and Geochem., Russ. Acad. of Sci., Novosibirsk.

Gravens, T. E., and A. I. Stewart (1978), Global morphology of nitric oxide in the lower *E* region, *J. Geophys. Res., 83*(A6), 2447.

Knyazev, A. K., L. B. Vanina, L. B. Korneeva, and V. N. Avdeev (1993), Specification of the empirical model of the electron concentration in the *D* region on the solar zenith angle using the rocket measurements, *Geomagn. Aeron.* (in Russian), *33*(5), 143.

McNamara, L. F. (1979), Statistical model of the *D* region, *Radio Sci., 14,* 1165.

Mechtly, E. A., M. M. Rao, D. O. Skaperdas, and L. G. Smith (1969), Latitude variations of the lower ionosphere, *Radio Sci., 4,* 517.

Nesterova, I. I., and E. I. Ginzburg (1985), *Catalog of the Electron Concentration Profiles* (in Russian), 211 pp., Inst. of Geol. and Geochem., Russ. Acad. of Sci., Novosibirsk.

Pancheva, D., and Pl. Mukhtarov (1997), Diurnal and seasonal variations of electron densities in the midlatitude *D* region, *J. Bulg. Geophys., 23*(1–2), 41.

Schwentek, H. (1976), Ionospheric absorption between 53°N and 53°S observed on board ship, *J. Atmos. Terr. Phys., 38*(14), 89.

Shirke, J. S., and G. W. Henry (1967), Geomagnetic anomaly in ionospheric absorption at low latitude observed on board USNS Croatan, *Ann. Geophys., 23,* 517.

G. V. Givishvili and R. V. Pisarev, Institute of Terrestrial Magnetism, Ionosphere, and Radio Wave Propagation, 192042 Troitsk, Moscow Region, Russia. (givi@izmiran.rssi.ru)